

# Measurement Method of Mass Flux and Concentration in Supersonic Mixing by Hot-Wire Anemometry

Akira KONDO\*, Shoji SAKAUE† and Takakage ARAI‡

\* Ph.D. student, JSPS research fellow, Dept. of Aerospace Engineering, Osaka Prefecture University, 1-1, Gakuen-cho, Naka-ku, Sakai, Osaka, Japan, kondoh@aero.osakafu-u.ac.jp

† Assistant Professor, Dept. of Aerospace Engineering, Osaka Prefecture University, 1-1, Gakuen-cho, Naka-ku, Sakai, Osaka, Japan, sakaue@aero.osakafu-u.ac.jp

‡ Professor, Dept. of Aerospace Engineering, Osaka Prefecture University, 1-1, Gakuen-cho, Naka-ku, Sakai, Osaka, Japan, arai@aero.osakafu-u.ac.jp

## ABSTRACT

In the present study, we made efforts to realize a measurement method of instantaneous fluctuations of mass flux and concentration with 500 kHz bandwidth to explain supersonic mixing process. In our method, by using double-hot-wire probe which has two kinds of wires with different responses to the variations of mass flux and concentration, we were able to explain the mixing flow field with the help of calibration maps of each wire. Experiments were carried out in a 2D supersonic air/helium mixing layer at the Mach number of 2.4. The results show that the proposed method is very effective for the analysis of supersonic mixing. However, in selection of each hot wire, its diameter and thermal conductivity, both should be considered.

## 1. INTRODUCTION

The supersonic combustion ramjet engine (SCRAMJET engine) is a candidate propulsion system for future space transportation or hypersonic vehicles [1]. The reason for supersonic combustion is to avoid the possible large total pressure loss and high static temperature rise that would be caused by the deceleration of the flow from hypersonic to subsonic. For typical operating conditions of scramjet, the time scale for complete combustion of the fuel hydrogen and the air oxygen will be on the order of 1 ms so that the problem of providing rapid mixing of molecular level is quintessential for the combustor design of SCRAMJET engine. Some injection schemes to enhance the mixing for the SCRAMJET engine have been reported in literature, such as wedge shaped injector schemes [2, 3, 4, 5], ramp-injector schemes [6, 7, 8, 9], and included-injector schemes [10, 11]. It is important to evaluate the mixing condition in the SCRAMJET engine in order to suggest or develop these injection schemes. Combustion is the phenomenon accomplished by molecular mixture of fuel and oxygen, such that the mixing condition is quantitatively evaluated by time series measurement of fuel concentration quantitatively. However, instantaneous measurement method has not been established yet. PLIF [6] and Mie scattering method [10] are restricted to measurement of mean characteristics of flow fields due to the laser repetition frequency. The suction probe proposed by Xillo et al. [12] has 2.5 kHz sampling frequency, which is insufficient for detection of the instantaneous mixing process in supersonic flow. Arai et al. [13] proposed an evaluation method with 100 kHz bandwidth, which had limitation due to its dependency on qualitative measurement. Here, we have proposed a quantitative measurement method for the instantaneous fluctuation of mass flux and concentration with 500 kHz bandwidth. Because our measurement method has extremely high time resolution, we can find flow structure whose scale is up to 1 mm in 500 m/s mixing flow field. As mentioned later in section 3.2, spatial resolution of our measurement method is also improved compared to that of Arai et al [13].

In the present study, in order to establish the instantaneous quantitative measurement method for mass flux and concentration of supersonic mixing flow field, we first resolved the problems in our measurement method; those were calibration method, consistency of the flows captured by two hot wires, and thermal lag of hot wire response. Next, to demonstrate the usefulness of our measurement method and to verify whether our method can be applied to time-series evaluation of supersonic

mixing, we carried out the fluctuation measurements of mass flux and concentration on 2D supersonic mixing layer.

## 2. PRINCIPLE OF MEASUREMENT METHOD

The principle of our measurement method is almost the same as that of Harion et al. [14] which is established in subsonic flow. Our device is composed of double-hot-wire probe shown in Fig. 1 and CVA (Constant Voltage Anemometer) circuit with 500 kHz bandwidth. For simultaneous measurements of mass flux and concentration, two kinds of hot wire with different characteristics of heat transfer must be used for the double-hot-wire probe.

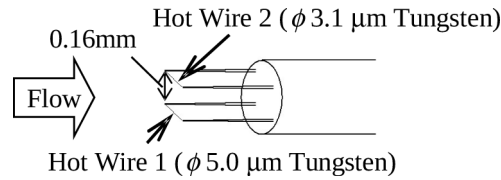


Figure 1. Double-hot-wire probe.

The heat balance of each wire is written as follows:

$$\frac{V_{wi}^2}{R_{wi}(R_{wi} - R_{ai})} = \frac{\pi l_i k_i}{\alpha_i R_f} (a_i(c) + b_i(c) \sqrt{Re_i}) \quad (i=1,2), \quad (1)$$

where  $V_w$  is the voltage across the hot wire,  $R_w$  is the resistance of the hot wire at the operating temperature  $T_w$ ,  $R_a$  is the resistance of the unheated wire at ambient temperature  $T_a$ ,  $l$  and  $k$  are the length and the thermal conductivity of the hot wire,  $Re$  is the Reynolds number based on the diameter of the hot wire  $d$ ,  $c$  is the concentration of the fuel gas, and subscript  $i$  denotes the ordinal number of hot wires. In this study, we used helium gas as pseudo fuel (air/hydrogen is ideal but safety concerns recommend air/helium instead).  $\alpha$  and  $R_{ref}$  are the temperature coefficient of resistance and the resistance of the wire at reference temperature  $T_{ref}$ , which are contained in the well known temperature-resistance relationship;  $R_w = R_{ref} [1 + \alpha (T_w - T_{ref})]$ .  $A_i(c)$  and  $B_i(c)$  are experimentally determined constants that vary with the concentration of the mixture. Left side of the eqn (1) indicates the power dissipation ratio ( $PDR$ ) of the hot wire. This equation can be simplified as follows:

$$PDR_i = A_i(c) + B_i(c) \sqrt{\rho u} \quad (i=1,2), \quad (2)$$

where,

$$A(c) = \frac{\pi l k}{\alpha R_f} a(c), \quad (3)$$

$$B(c) = \frac{\pi l k}{\alpha R_f} \sqrt{\frac{d}{\mu}} b(c), \quad (4)$$

$\rho u$  is the mass flux, and  $\mu$  is the coefficient of viscosity. Eliminating the square root of the mass flux from eqn (2), we obtain the following iso-concentration equation:

$$PDR_1 = \frac{B_1(c)}{B_2(c)} PDR_2 + A_1(c) - \frac{B_1(c)}{B_2(c)} A_2(c). \quad (5)$$

Substituting the measured  $PDR_i$  into eqn (5), the helium concentration  $c$  can be detected and the mass flux  $\rho u$  can be obtained from eqn (2).

## 3. PROBLEMS OF THE MEASUREMENT METHOD

In our measurement method for the investigation of the instantaneous mixing process in supersonic flow, three problems were encountered, namely calibration method, consistency of the flows captured by the two wires and thermal lag of hot wire response. In order to resolve these problems, we carried out the following experiments.

### 3.1 Calibration Method

The coefficients  $A_i(c)$  and  $B_i(c)$  in eqn (2) must be determined by the hot wire calibration for mass flux  $\rho u$  and concentration  $c$ . It is desirable that the hot wire is calibrated for the wide variations of mass flux and concentration by as small amount of mixed gas as possible. For that reason, we used the sonic nozzle calibration apparatus as shown in Fig. 2. Air/helium mixed gas is blown down through the circular convergent nozzle whose exit diameter is 5 mm, and the hot wire is calibrated at the nozzle exit where the speed of mixed gas reaches Mach 1.0. The mass flux at the nozzle exit can easily be evaluated from the chamber pressure and temperature. By using the sonic nozzle apparatus, we can calibrate the hot wire for the wide variations of mass flux by the small amount of the mixed gas.

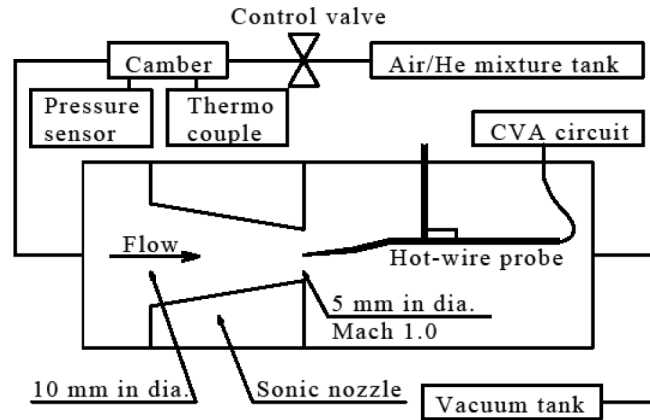


Figure 2. Sonic nozzle calibration apparatus.

The fluid temperature  $T_a$  of the sonic flow at the nozzle exit is different from that in supersonic flow. Therefore, it must be confirmed that the calibration results by using sonic nozzle apparatus can be applied to the measurements in supersonic flow. To compare with sonic nozzle calibration result, calibration was also conducted in supersonic turbulent boundary layer at Mach 2.4. Mass flux was calculated from following equations by using the pitot pressure by supposing that wall is adiabatic, differential of static pressure  $\partial p/\partial y$  is zero across the boundary layer, and normal shock expression can be used near the tip of the pitot probe. Mach number of the free stream,  $M_\infty$ , is obtained from the equation as follows:

$$\frac{P_{pitot,\infty}}{P_0} = \left\{ \frac{2\gamma}{\gamma+1} M_\infty^2 - \frac{\gamma-1}{\gamma+1} \right\}^{\frac{-1}{\gamma-1}} \left\{ \frac{(\gamma-1)M_\infty^2/2 + 1}{(\gamma+1)M_\infty^2/2} \right\}^{\frac{-\gamma}{\gamma-1}}, \quad (6)$$

where,  $P_{pitot,\infty}$  is the pitot pressure at free stream,  $P_0$  is total pressure at free stream, and  $\gamma$  is specific heat ratio. By using the free stream Mach number  $M_\infty$ , static pressure  $P$  is obtained as follows:

$$\frac{P}{P_0} = \left( 1 + \frac{\gamma-1}{2} M_\infty^2 \right)^{\frac{-\gamma}{\gamma-1}}. \quad (7)$$

Thus, we can obtain the Mach number  $M$  distribution across the turbulent boundary layer by using static pressure  $P$  and measured pitot pressure  $P_{pitot}$ :

$$\frac{P_{pitot}}{P} = \left( \frac{\gamma+1}{2} M^2 \right)^{\frac{\gamma}{\gamma-1}} \left\{ \frac{(\gamma+1)}{2\gamma M^2 - (\gamma-1)} \right\}^{\frac{1}{\gamma-1}} \text{ for } M > 1, \quad (8)$$

$$\frac{P}{P_{pitot}} = \left( 1 + \frac{\gamma+1}{2} M^2 \right)^{\frac{-\gamma}{\gamma-1}} \text{ for } M \leq 1. \quad (9)$$

Using Mach number  $M$ , Mass flux  $\rho u$  is obtained as following:

$$\rho u = \left\{ \rho_0 P_0 \frac{2\gamma M^2}{2 + (\gamma - 1)M^2} \right\}^{\frac{1}{2}} \left( 1 + \frac{\gamma - 1}{2} M^2 \right)^{-\frac{1}{\gamma - 1}}, \quad (10)$$

where,  $\rho_0$  is total density at free stream. Hot wire output can be associated with mass flux by hot wire measurement at the same point of pitot tube measurement.

Figure 3 shows the comparison between the calibration results for air flow ( $c = 0$ ) by using the sonic nozzle and in the supersonic turbulent boundary layer at Mach 2.4. As seen from Fig. 3, both results are in good agreement. The correlation coefficient between the each calibration results was 0.997 implying that the calibration results of the sonic nozzle can be applied to the supersonic flow measurements.

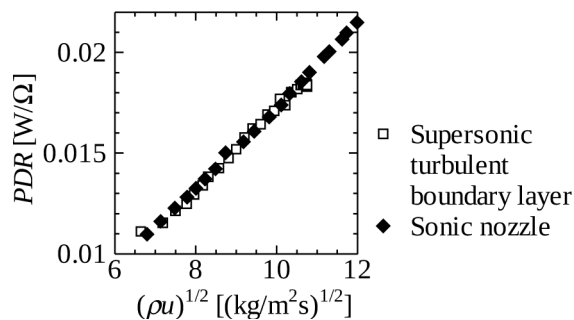


Figure 3. Calibration results in sonic flow and in Mach 2.4 supersonic turbulent boundary layer flow.

### 3.2 Flow Consistency

As seen from the eqn (2), each hot wire of the double-hot-wire probe must capture the same flow in our measurement method. The each hot wire cannot capture the flow at the same point due to its configuration, therefore, the distance between the two wires must be minimized as much as possible. A double-hot-wire probe with 0.16mm gap between its wires, as shown in Fig. 1, was constructed for the present study. Arai et al [13] used a double hot wire probe with a 1.5 mm gap between its wires. Thus the resolution of the present probe is ten times better than that of Arai et al [13]. Our measurement method has 500 kHz bandwidth, the scale of the flow structure captured by hot wire is up to 1 mm in the flow field whose velocity is 500 m/s. Therefore, the distance between the two hot wires must be less than 1 mm at least. Because of the fine resolution of the probe used in the present study, the measurement errors are expected to be rather negligibly small.

To confirm the flow consistency captured by the two hot wires, we measured the Mach 2.4 supersonic flow with two pairs of counter rotating streamwise vortices, as shown in Fig. 4 whose configuration simulates one of the ramp injector. The use of large-scale streamwise vortices is effective for the supersonic mixing enhancement [15]. The hot wire measurements were carried out at  $x = 100$  mm,  $2 \text{ mm} \leq y \leq 14$  mm,  $z = 15$  mm by using the double-hot-wire probe. Figure 5 shows the instantaneous schlieren photograph of the flow field. The broken line indicates upper side of the streamwise vortices. Streamwise vortices are grown up toward downstream just behind the ramp. At  $x = 100$  mm, the streamwise vortices are fully developed and start to breakdown to small scale turbulent eddies of high mixing power [15]. To avoid the influence of thermal lag of hot wire, discussed below, the same tungsten wires whose length and diameter were 0.5 mm and 5  $\mu\text{m}$  was used. Figure 6 shows the correlation coefficients between the each hot wire output. The correlation coefficients at  $5 \text{ mm} \leq y \leq 13$  mm were about 0.9, so that we can confirm that the flow captured by the two wires is almost the same. However, the correlation changes for the worse at  $y < 5$  mm and  $y = 14$  mm. At  $x = 100$  mm, the shock wave reflecting on the channel lower wall passed through at  $y = 5$  mm. The streamwise vortices passing through the shock wave is expected to break down into

small eddies. The consistency captured by the two hot wires became worse because of the small scale of the flow structures considering the probe configuration. Meanwhile, at  $x = 100$  mm, the streamwise vortices developed up to  $y = 13$  mm and the turbulent boundary layer formed on the upper wall at  $y \geq 16$  mm. Figure 7 shows power spectra of measurement result and electrical noise at  $y = 6$  mm (in the streamwise vortices) and 14 mm (in the free stream). Power spectrum of  $y = 14$  mm is lower than that of  $y = 6$  mm. This indicates that signal to noise ratio at  $y = 14$  mm is worse than that at  $y = 6$  mm. Thus, the consistency captured by the two hot wires became worse because of the electrical noise which cannot be negligible in the signal. In conclusion, the two hot wires can capture almost the same flow, but it is necessary to pay attention to the scale of the flow structures and the electrical noise level.

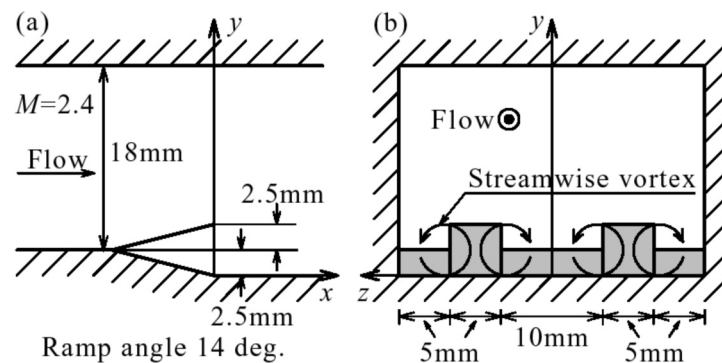


Figure 4. Schematic of wall-mounted device generating two pairs of counter-rotating streamwise vortices and coordinate system: (a)  $xy$  cross section, (b)  $yz$  cross section.

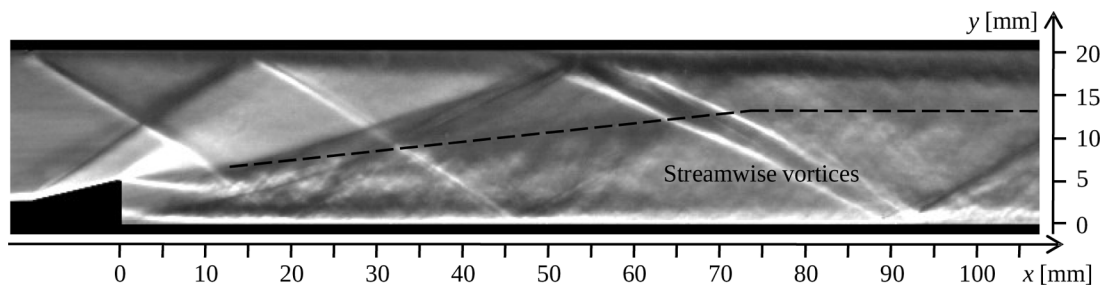


Figure 5. Instantaneous schlieren photograph of Mach 2.4 supersonic flow with streamwise vortices. Knife edge is set at lower side. Broken line indicates upper side of streamwise vortices.

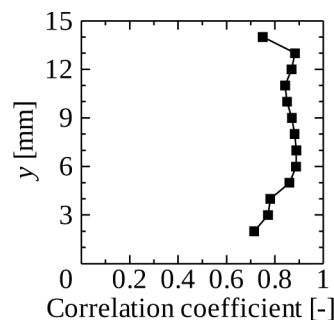


Figure 6. Correlation coefficients between each hot-wire output voltage (at  $x = 100$  mm).

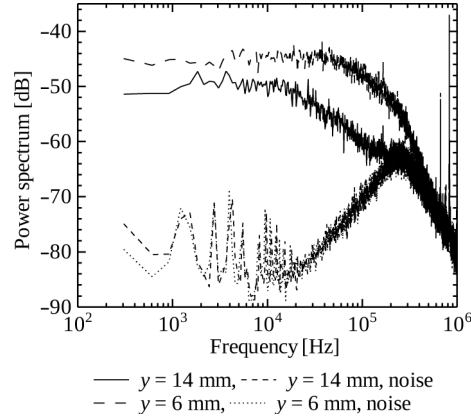


Figure 7. Power spectra of measurement results and electric noise at  $y = 6$  mm and 14 mm.

### 3.3 Thermal Lag Compensation

Hot wire responses with first order lag to the fluctuations of the flow due to its heat inertia. For that reason, hot wire output must be compensated properly. The time constant of the hot wire response changes according to the flow condition. When CVA circuit is used, thermal lags of each wire can be compensated by the software processing method [16].

It is well known that the resistance of the hot wire depends on temperature:

$$R_w = R_{ref} [1 + \alpha (T_w - T_{ref})]. \quad (11)$$

The time constant  $T$  of the hot wire by using the basic CVA circuit is written as follows:

$$T = \frac{a_w}{2a_w + 1} \frac{C_w}{R_{ref}} \frac{1}{I_w^2}, \quad (12)$$

where  $a_w$  is the overheat ratio,  $C_w$  is the heat capacity of the hot wire,  $I_w$  is the current through the wire, and  $R_{ref}$  is the resistance of the unheated wire at reference temperature  $T_{ref}$ .  $C_w/\alpha R_{ref}$  is the constant value peculiar to the each wire.  $a_w$  and  $I_w$  can be determined by measurement. The time constant of the hot wire can be determined by eqn (12) if  $C_w/\alpha R_{ref}$  is known.

The relation between the ideal hot wire response  $v_{ideal}$ , which has no thermal lag, and the raw hot wire response  $v_{raw}$ , which has first order lag by the heat inertia, is follows:

$$v_{ideal} = v_{raw} + T \frac{dv_{raw}}{dt}. \quad (13)$$

Laplace transform of both sides of eqn (13) is

$$V_{raw} = \frac{1}{1 + Ts} V_{ideal}. \quad (14)$$

If square wave is the input, the response  $V_{ideal}$  must be the form of a square wave. Therefore eqn (14) can be rewritten in the form:

$$V_{raw} = \frac{1}{1 + Ts} \frac{K}{s}, \quad (15)$$

where  $K$  is a constant. Consequently the response  $v_{raw}$  for the square input is obtained by inverse laplace transform of eqn (15):

$$v_{raw} = K \left( 1 - e^{-\frac{t}{T}} \right). \quad (16)$$

When the time  $t = T$ , eqn (16) can be rewritten in the form:

$$v_{raw}(T) = K (1 - e^{-1}) \cong 0.632K. \quad (17)$$

Figure 8 shows the typical response of the first order lag of the hot wire to the input square wave. As seen from eqn (17), the time constant of the wire can be determined as the time to reach the 63.2% of the final value  $K$ , and  $C_w/\rho R_{ref}$  is obtained by substituting the time constant to eqn (12).

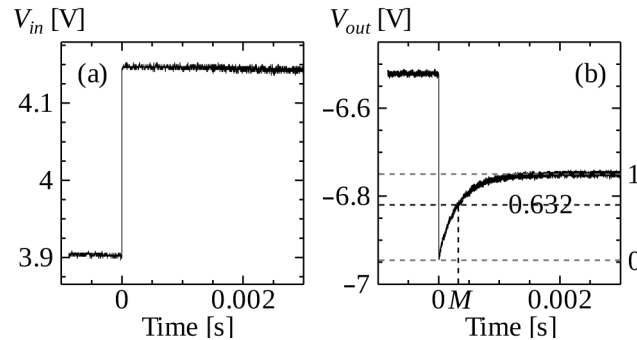


Figure 8. Input signal and first order lag response of hot wire anemometry output voltage: (a) square wave input, (b) first order lag response.

#### 4. MEASUREMENTS IN MIXING LAYER

##### 4.1 Calibration for Concentration and Mass Flux

In the present study, two kinds of tungsten wires were used for the double-hot-wire probe, their diameter were 5  $\mu\text{m}$  and 3.1  $\mu\text{m}$ , respectively. The hot wires were calibrated for five kinds of air/helium mixed gas whose helium concentrations were 0%, 20%, 40%, 60%, and 100%. Figure 9 shows the calibration results of the each wire by using sonic nozzle calibration apparatus as mentioned above. From these results, the coefficients  $A_i(c)$  and  $B_i(c)$  in eqn (2) were determined for each of helium concentrations.  $A_i(c)$  and  $B_i(c)$  were determined as cubic functions of helium concentration, as shown in Fig. 10. Figure 11 shows the calibration map of eqn (5) by using  $A_i(c)$  and  $B_i(c)$  of cubic functions of helium concentration shown in Fig. 10.

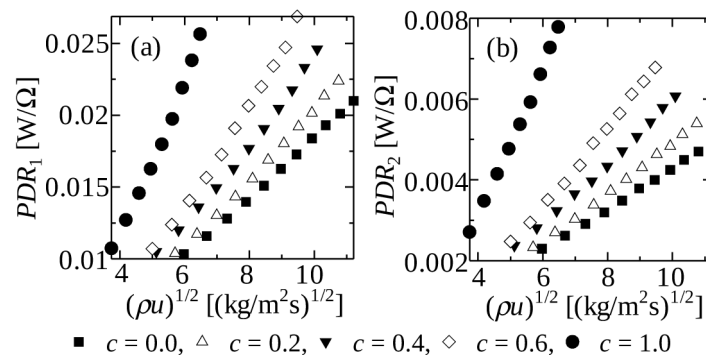


Figure 9. Calibration results for helium concentration and mass flux: (a)  $\phi$  5  $\mu\text{m}$  tungsten wire, (b)  $\phi$  3.1  $\mu\text{m}$  tungsten wire.

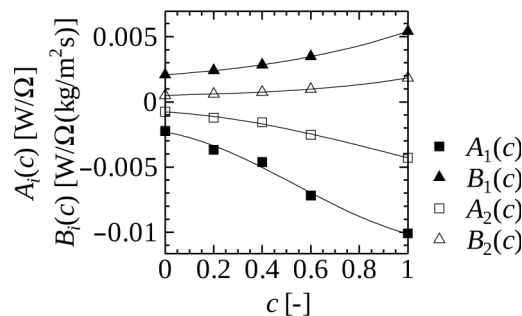


Figure 10.  $A_i(c)$  and  $B_i(c)$  determined by Fig. 9. Each line indicates cubic approximation for helium concentration.

In order to estimate the error involved in our measurement method, the measurement values were compared with the actual values of mass flux and helium concentration as shown in Fig. 12. The measurement value means the value calculated from  $PDR$  of each hot wire by using the calibration map as shown in Fig. 11. The actual value is calculated by using the helium concentration of air/helium mixed gas and the chamber pressure and temperature. As seen from Fig. 12, it is found that the error in this method was less than  $\pm 10\%$ . However, in the small  $PDR$  region where the iso-concentration lines were close to each other, the measurement error is quite large. In this region, heat transfer becomes small because of the small mass flux condition, so that the variation of  $PDR$  for the helium concentration becomes smaller than the large  $PDR$  region.

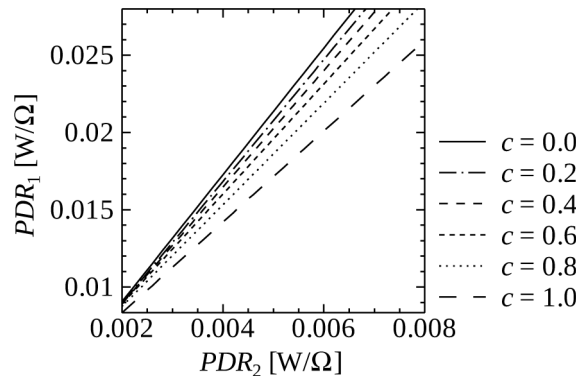


Figure 11. Calibration map used for detecting helium concentration.

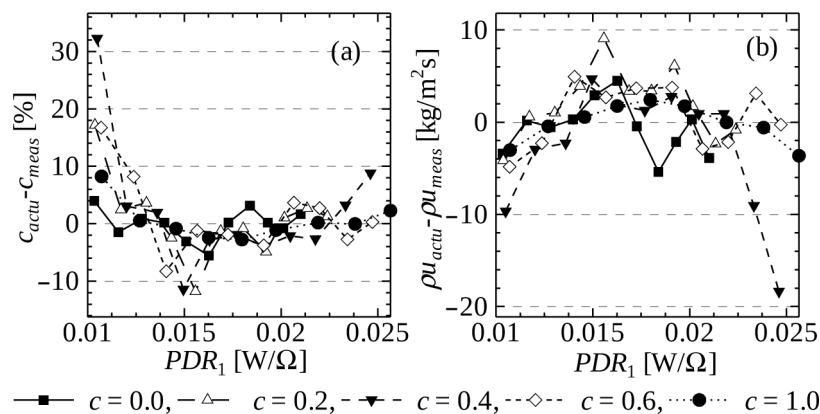


Figure 12. Difference between measurement value and actual value:  
(a) helium concentration, (b) mass flux.

#### 4.2 Results and Discussions

In order to demonstrate the usefulness and to examine the accuracy of our method, we applied our method to the measurement of two dimensional air/helium mixing layer as shown in Fig. 13. Air and helium flow, whose Mach numbers were 2.4 and 0.4 respectively, were separated by a thin splitter plate and the mixing layer was generated downstream of the splitter plate. The length of the test section was 400 mm, the height was 35.5 mm, and the width was 30 mm. Figure 14 shows the instantaneous schlieren photographs of the mixing layer just behind the splitter plate. It can be seen that the supersonic mixing layer is developing in the downstream. The measurements were conducted at  $x = 30$  mm and  $x = 100$  mm,  $-4$  mm  $\leq y \leq 10$  mm, and  $z = 15$  mm by using calibrated double-hot-wire probe mentioned above.

Figure 15 shows the mass flux and the helium concentration profiles of the mixing layer. Solid lines and broken lines indicate the profiles at  $x = 30$  mm and at  $x = 100$  mm, respectively. At these two stations, air and helium do mix only at the center region of the mixing layer as seen from the schlieren photographs shown in Fig. 14. The helium concentration must be zero at the upper side of the mixing layer and must be one at the lower side of the mixing layer. However, the results of the helium concentration are inconsistent, especially at the lower side of the mixing layer. Figure 16 plots the

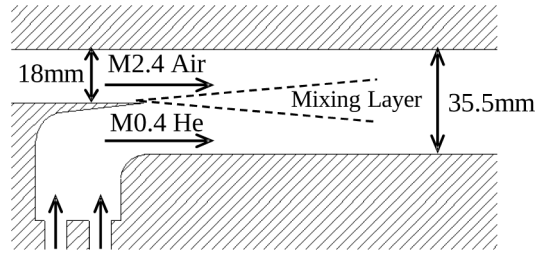


Figure 13. Schematic of the mixing layer.

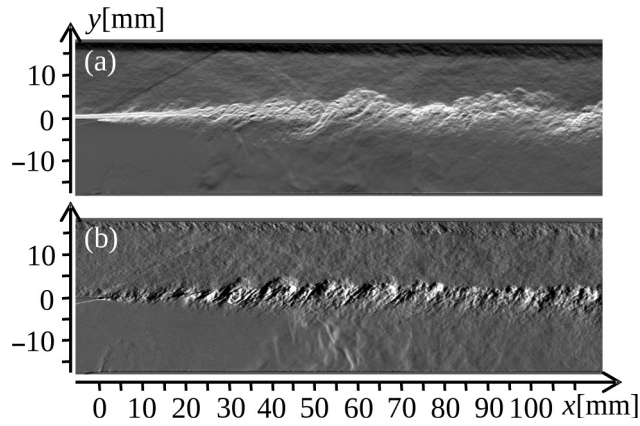


Figure 14. Instantaneous schlieren photographs of the mixing layer: (a) knife edge: lower position, (b) knife edge: left.

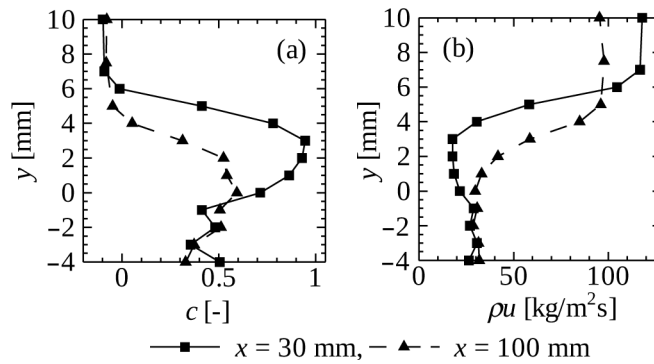


Figure 15. y-directions of mean helium concentration and mass flux in the mixing layer: (a) mean helium concentration, (b) mean mass flux.

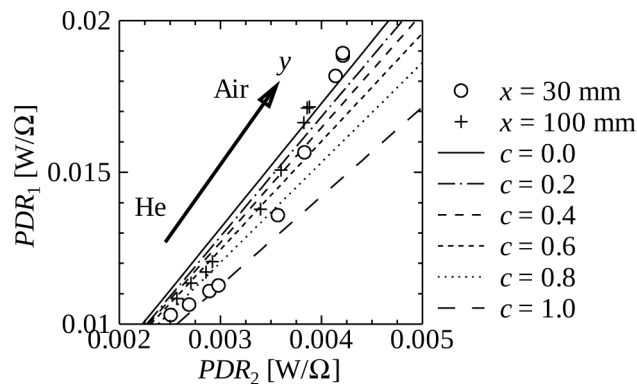


Figure 16. Measurement results of the mixing layer plotted on the calibration map of Fig.11.

results of Fig. 15 on the calibration map of Fig. 11. In the lower side of the mixing layer, the power dissipation ratios of each hot wire were extremely small and the iso-concentration lines were close to each other as mentioned above. Therefore, the results could not be estimated correctly in this region.

This can be improved if we select more proper material as the hot wire. To improve the measurement accuracy, the rate of change of the slope and the intercept in eqn(2) with respect to concentration

$$\text{Slope } \frac{\partial}{\partial c} \left( \frac{B_1(c)}{B_2(c)} \right) = \frac{\alpha_2 k_1}{\alpha_1 k_2} \sqrt{\frac{d_1}{d_2}} \frac{\partial}{\partial c} \left( \frac{b_1(c)}{b_2(c)} \right), \quad (18)$$

$$\text{Intercept } \frac{\partial}{\partial c} \left( A_1(c) - A_2(c) \frac{B_1(c)}{B_2(c)} \right) = \frac{\pi l_1 k_1}{\alpha R_f} \left\{ \frac{\partial a_1(c)}{\partial c} - \sqrt{\frac{d_1}{d_2}} \frac{\partial}{\partial c} \left( a_2(c) \frac{b_1(c)}{b_2(c)} \right) \right\}, \quad (19)$$

must be enlarge. Where, the length of the each wire  $l_i$  is assumed the same. Partial differential of the calibration constants of  $a_i(c)$  and  $b_i(c)$  cannot be written definitely; however, it is found that ratio of the temperature coefficient of resistance  $\alpha_2/\alpha_1$ , thermal conductivity  $k_1/k_2$ , and square root of hot wire diameter  $(d_1/d_2)^{0.5}$  are related to the rate of change of the slope and the intercept with respect to concentration. In the case that  $\phi 5 \text{ mm}$  and  $\phi 3.1 \text{ mm}$  tungsten wire are used as the double hot wire,  $(d_1/d_2)^{0.5}$  is 1.27, and  $(a_2/a_1) \times (k_1/k_2) \times (d_1/d_2)^{0.5}$  is also 1.27 (because of the same material), respectively. Figure 17 shows an example of the calibration map that  $\phi 5 \text{ }\mu\text{m}$  tungsten wire and  $\phi 5 \text{ }\mu\text{m}$  platinum wire are used as the double hot wire. In this case,  $(d_1/d_2)^{0.5}$  is 1.0, and  $(a_2/a_1) \times (k_1/k_2) \times (d_1/d_2)^{0.5}$  is 1.79, respectively. As seen from Fig. 17, it is found that each iso-concentration line is mutually away, so that the concentration and mass flux can be also obtained by using different characteristics of wires even if the diameter of the wires is the same. Meanwhile, the aerodynamic load on hot wire is quite large in supersonic flow. For that reason, the platinum wire cannot be used because its strength is not enough. Consequently, to improve measurement accuracy, wire materials must be

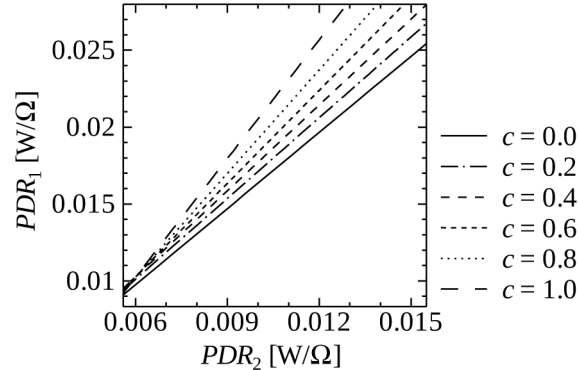


Figure 17 Calibration map in the case that  $\phi 5 \text{ }\mu\text{m}$  tungsten wire and  $\phi 5 \text{ }\mu\text{m}$  platinum wire are used as the double hot wire.

selected by not only the difference of the thermal conductivity and wire diameter of each wire but also sufficient wire strength for measurement in supersonic flow.

## 5. CONCLUSIONS

In the present study, we proposed simultaneous quantitation method of fluctuating mass flux and concentration. At first we resolve three problems in this method; those are calibration method, consistency of the flows captured by two hot wires, and thermal lag of hot-wire response. We figured out that we must pay attention to the effect of the scale of the flow structures and the electric noise level for good consistency of the flow which each hot wire capture. Next, hot wire calibration for mass flux and concentration was conducted by using sonic nozzle facility, and we confirmed the capability of the measurement of mass flux and concentration separately. In addition, it is found that

the error in our method was less than 10%. Finally, to demonstrate the usefulness of our method, we measured the supersonic air/helium mixing layer by using this method. Thorough out this study, we showed that it was possible to measure fluctuating mass flux and concentration separately by using our measurement method. However, the measurement error becomes large at the small PDR region. To improve measurement accuracy in particular at the small PDR region, each hot wire material must be selected by not only the difference of thermal conductivity and wire diameter but also sufficient wire strength.

#### ACKNOWLEDGEMENTS

The present research was supported, in part, JSPS, Grant-in-Aid for Scientific Research, 1760694, 2005-2006, and 20560739, 2008-2010.

#### REFERENCES

- [1] Scuderi, L.F., Orton, G.F., Hunt, J.L., Mach 10 cruise/space access vehicle definition, AIAA-1998-1584, *AIAA Space Planes and Hypersonic Systems and Technologies Conference*, 1998.
- [2] Barber, M.J., Schelz, J.A., Roe, L.A., Normal, sonic helium injection through a wedge-shaped orifice into supersonic flow, *Journal of Propulsion and Power*, 1997, **13**(2), 257–263.
- [3] Sakima, F., Arai, T., Kasahara, J., Murakoshi, M., Ami, T., He, F., Sugiyama, H., Mixing of a hydrogen jet from a wedge shaped injector into a supersonic cross flow, *Transactions of the Japan Society for Aeronautical and Space Sciences*, 2004, **47**(154), 217–223.
- [4] Tomioka, S., Jacobsen, L.S., Schetz, J.A., Interaction between a supersonic airstream and a sonic jet injected through a diamond-shaped orifice, *38th Aerospace Sciences Meeting and Exhibit*, 2000.
- [5] Motogi, T., Shiratori, T., Sakurai, C., Experimental research on helium gas injection from a flat plate in supersonic flow (estimation on difference of injector shape), *Proceedings of the 39th Conference on Aerospace Propulsion*, 1999, 371–376 (in Japanese).
- [6] Donohue, J.M., McDaniel Jr., J.C., Complete three-dimensional multiparameter mapping of a supersonic ramp fuel injector flowfield, *AIAA Journal*, 1996, **34**(3), 455–462.
- [7] Morita, S., Arai, T., Nagata, H., Hosokawa, H., Sugiyama, H., Enhancement of supersonic mixing by backward facing step with ramp partially (evaluation of mixing condition using catalytic reaction on constant temperature Pt wire), *Proceedings of the 38th Conference on Aerospace Propulsion and the 8th Symposium on RAM/SCRAMJETS*, 1998, 33–35 (in Japanese).
- [8] Sunami, T., Breakdown process of supersonic streamwise vortices in spanwise-row configuration, *Nagare Journal of Japan Society of Fluid Mechanics*, 1999, **18**, 136–139 (in Japanese).
- [9] Wilson, M.P., Bowersox, R.D.W., Glawe, D.D., Experimental investigation of the role of downstream ramps on a supersonic injection plume, *Journal of Propulsion and Power*, 1999, **15**(3), 432–439.
- [10] Gruber, M.R., Nejad, A.S., Chen, T.H., Dutton, J.C., Mixing and penetration studies of sonic jets in a Mach 2 freestream, *Journal of Propulsion and Power*, 1995, **11**(2), 315–323.
- [11] Arai, T., Hukuzoe, H., Miura, J., Nagata, H., Hosokawa, H., Experimental investigation of inclined hydrogen injection into a supersonic flow, AIAA-1999-4915, *AIAA Space Planes and Hypersonic Systems and Technologies Conference*, 1998.
- [12] Xillo O.C., Schetz J.A., Ng W.F., and Simpson R.L., *A Sampling Probe for Fluctuating Concentration Measurement in Supersonic Flow*, M. S. thesis, Virginia Polytechnic Institute and State University, Blacksburg, 1998.
- [13] Arai T., Mizobata K., Minato R., Tanatugu N., Mori Y., and Kudo T., Correlation between Fluctuations of Mass Flux and Hydrogen Concentration in Supersonic Mixing, AIAA-2005-323, *AIAA/CIRA 13th International Space Planes and Hypersonics Systems and Technologies Conference*, 2005.
- [14] Harion J.L., Favre-Marinet M., Camano B., An Improved Method for Measureing Velocity and Concentration by Thermo-Anemometry in Turbulent helium-air mixtures, *Experiments in Fluid*, 1996, **22**(2), 174–182.

- [15] Arai T., Sakaue S., Morisaki T., KondoA., Hiejima T., and Nishioka M., Supersonic streamwise vortices breakdown in scramjet combustor, AIAA-2006-8025, *14th AIAA/AHI International Space Planes and Hypersonic Systems and Technologies Conference*, 2006.
- [16] Sarma G.R., Transfer function analysis of the constant voltage anemometer, *Review of Scientific Instruments*, 1998, 69(6), 2385-2391.